Electronic Supplementary Material (ESI) for Nanoscale.
This journal is © The Royal Society of Chemistry 2015

**Supplemental information**

# Antisite Defects in Layered Multiferroic $CuCr_{0.9}In_{0.1}P_2S_6$

Qian He,[1,*] Alex Belianinov,[2] Andrius Dziaugys,[3] Petro Maksymovych,[2] Yulian Vysochanskii,[4] Sergei V. Kalinin[2] and Albina Y. Borisevich[1,2,*]

[1] Materials Science and Technology Division, Oak Ridge National Laboratory, Oak Ridge, Tennessee, 37831, United States.

[2] The Institute for Functional Imaging of Materials and the Center for Nanophase Materials Sciences, Oak Ridge National Laboratory, Oak Ridge, Tennessee, 37831, United States.

[3] Department of Radiophysics, Faculty of Physics, Vilnius University, 2600, Lithuania

[4] Institute of Solid State Physics and Chemistry, Uzhgorod University, Uzhgorod, Ukraine 88000

* Corresponding authors (Qian He: heqian.lehigh@gmail.com; Albina Borisevich: albinab@ornl.gov)

## Materials and Methods:

### Sample Growth:

The crystalline samples of $CuInP_2S_6$ system were prepared by chemical transportation reaction using the elements in the stoichiometric proportions as previously described [1]. The resulting product has the form of thin plates with c-axis normal to the surface. The plate-like lamellae, $CuCr_{0.9}In_{0.1}P_2S_6$ crystals were grown at Uzghorod University, Ukraine.

### Thin film preparation:

Ultra-thin flakes of the compounds were obtained using the micromechanical cleaving, also known as the “Scotch tape method”, which is widely used for preparing 2D materials such as graphene. All

operations were performed in a clean room; CITP was exfoliated 2-3 times by the scotch tape, in order to obtain fresh surfaces of the compound. Next the sample containing tape was firmly pressed against the preprocessed $SiO_2$/Si wafer, and then the tape was gently peeled away so that some exfoliated film flakes were left on the substrate. The $SiO_2$ layer on the wafer was ~300 nm, which is originally optimized for visualizing single layer graphene with white light. The apparent color of the compound with different thickness was then calibrated with AFM measurement and used to quickly locate thin layers.

**STEM:**

In order to obtain a specimen for TEM characterization, a Quantifoil® holey carbon Au grid was attached to the target thin flake via the solvent surface tension of Isopropyl alcohol (IPA), and then isolated by etching away the underneath $SiO_2$ layer by buffered HF. STEM characterization was done using the Nion UltraSTEM 200 operated at 200kV at Oak Ridge National Labs. The image intensity analysis was done using Gatan Digital Micrograph. Image simulation was done using the Kirkland's multi-slice frozen phonon code.[2]

**AFM:**

Thickness measurement were performed on a Cypher AFM provided by Asylum Research. Samples were mounted using silver paste (Ted Pella Prod. No. 16035) to metal disks (Ted Pella Prod. No. 16218); with a grounding wire soldered directly on to the disk.

References:

1. Belianinov, A. *et al.* CuInP2S6 Room Temperature Layered Ferroelectric. *Nano Lett.* **15,** 3808–14 (2015).

2. Kirkland, E. J. *Advanced Computing in Electron Microscopy*. (Springer Science & Business Media, 2010). at <https://books.google.com/books?id=YscLlyaiNvoC&pgis=1>

**additional Figures**

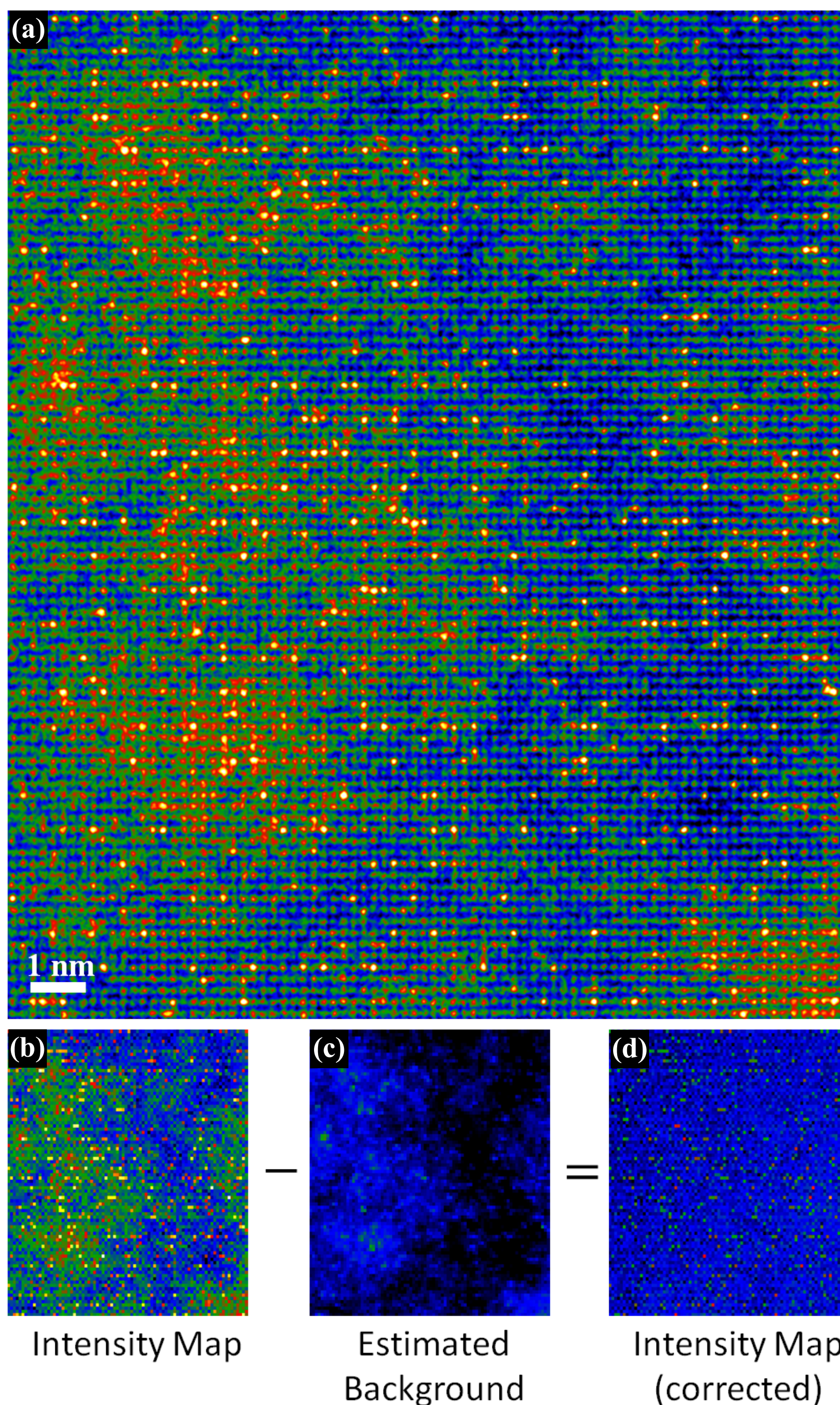


Figure S1. (a) The STEM-HAADF image of the 8-layer $CuCr_{0.9}In_{0.1}P_2S_6$ flake with $87 \times 84 = 7308$ atom columns in the field of view. (b) Atom column intensity map extracted from image *(a)*, using the center of mass peak finding algorithm. (c) Image background due to hydrocarbon

contamination estimated from adjacent vacuum sites for each column. (d) Background corrected atom column intensity map for further analysis.

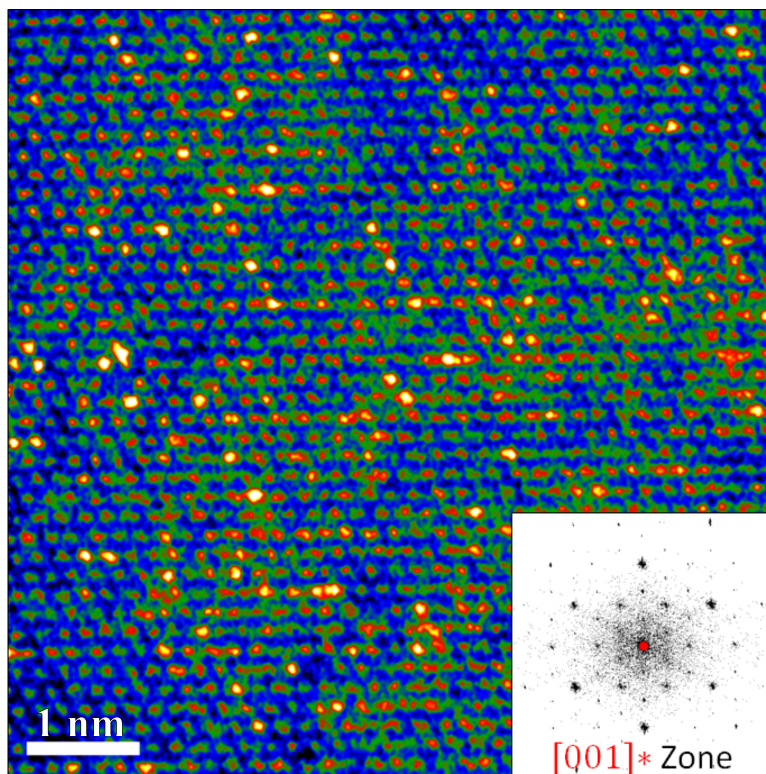


Figure S2. STEM-HAADF image of the 8-layer $CuCr_{0.9}In_{0.1}P_2S_6$ viewed at the ab-plane ([001]* zone, the plane normal direction). The specimen is bent so that different orientations can be observed without actually tilting the specimen.

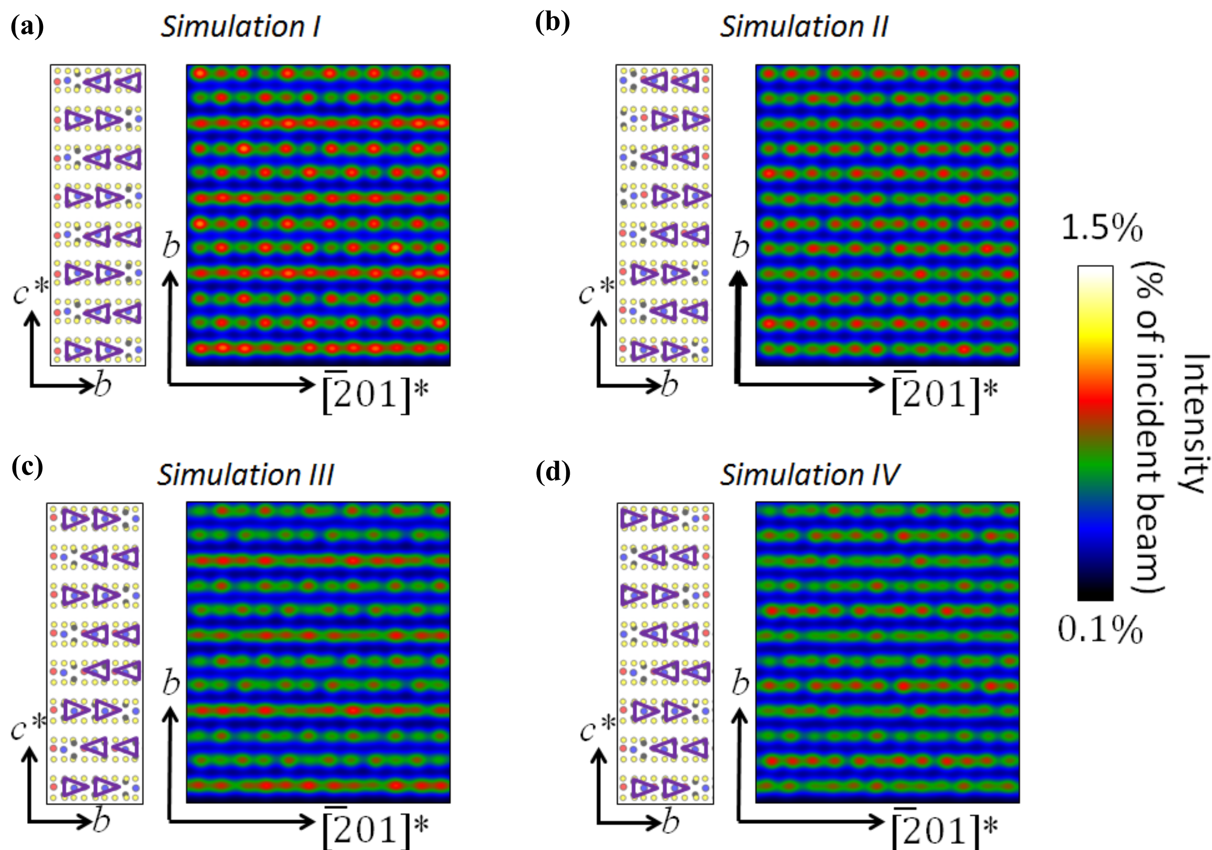


Figure S3. Multislice HAADF image simulations of $CuCrP_2S_6$ crystal with (a) ideal structure and (b-d) different stacking fault configurations. The side view models are shown in the left column and resultant simulated image viewed through [102] zone are shown in the right column. The stacking faults structure are built as follows: The bottom four layers of all four structures are the same. The top 4 layers (b) shift $1/3\vec{b}$, (c) rotate 180° around a Cu site and (d) rotate 180° around a Cu site plus shift $1/3\vec{b}$. Purple triangles are plotted from the P2 sites toward the Cu site, in order to highlight the stacking sequence.

In the experimental data (Figure 3), the mean intensities for column A, B and C the 0.098 $\pm 0.001$, $0.097 \pm 0.001$ and $0.077 \pm 0.001$ respectively, with 99.9% confidence intervals. Since we normalize all the intensities, these translate to $100 \pm 1\%$, $99 \pm 1\%$ and $79 \pm 1\%$. As shown in Figure S4, the experimental data is in close agreement with the image simulation results of the case of normal stacking (Simulation I), where Cu-Cu and $P_2$-$P_2$ columns have almost identical intensity and Cr-Cr column gives much lower intensity.

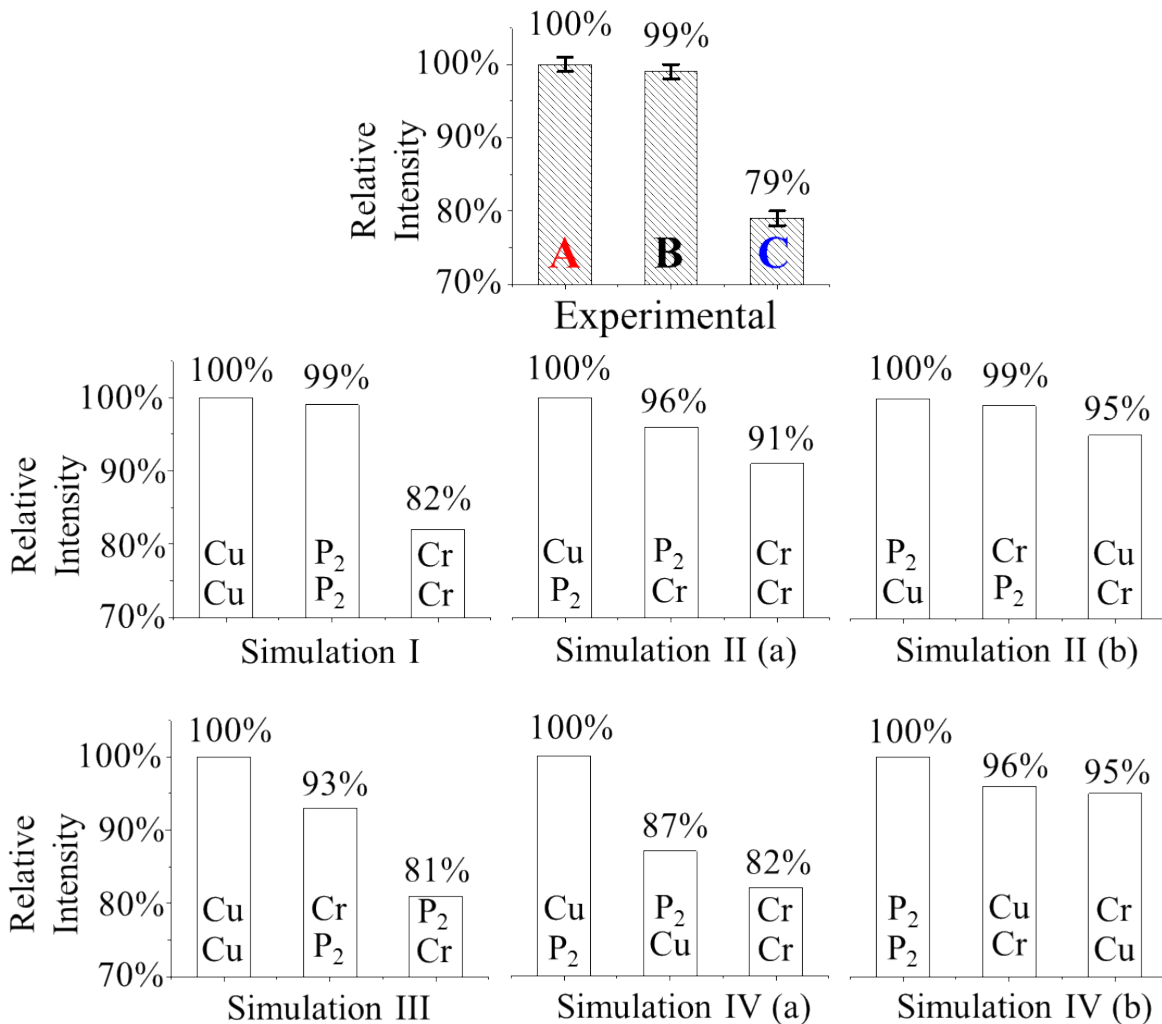

Figure S4 Column mean intensities obtained from experimental data shown in Figure 3 and simulation results shown in Figure S3. All 6 possible configurations of stacking two layers of Cu – $P_2$ – Cr are obtained from four simulations shown in Figure S4. All the column mean intensities are re-normalized to the brightest columns in each case. The experimental data matches the best with the Simulation I, suggesting there are no stacking faults present. We can therefore assign the blue columns C in Figure 3 to be Cr. With further assumption that In is not going to substitute two P atoms to alter the $P_2S_6$ framework, red columns A and black columns B in Figure 3 can be assigned to be Cu and $P_2$ respectively.